Multiple Gateway Transmit Diversity in Q/V Band Feeder Links

Ahmad Gharanjik, *Student Member, IEEE,* Bhavani Shankar M. R., *Member, IEEE,* Pantelis-Daniel Arapoglou, and Björn Ottersten, *Fellow, IEEE*

Abstract—Design of high bandwidth and reliable feeder links is central towards provisioning new services on the user link of a multibeam satellite communication (SatCom) system. Towards this, utilization of the Q/V band and an exploitation of multiple gateways (GW) as a transmit diversity measure for overcoming severe propagation effects are being considered. In this context, this contribution deals with the design of a feeder link comprising $N + P$ GWs (N active and P redundant GWs). Towards provisioning the desired availability, a novel switching scheme is analysed and practical aspects such as prediction based switching and switching rate are discussed. Unlike most relevant works, a dynamic rain attenuation model is used to derive analytically average outage probability in the fundamental $1 + 1$ gateway case. Building on this result, an analysis for the $N + P$ scenario leading to a quantification of the end−to−end performance is provided. This analysis aids system sizing by illustrating the interplay between the number of active and redundant gateways on the chosen metrics : average outage and average switching rate.

Index Terms—Gateway Diversity, $N + P$ scheme, Feeder Link, Q/V Band, Satellite Communication, Rain Attenuation.

I. INTRODUCTION

DEMANDS for broadband data services are increasing dramatically every year. Although, satellite solutions have the advantage of covering these demands over a wide geography, it is necessary to push the limits of the offered capacity in view of the competition from terrestrial solutions. Current high throughput satellite systems have capacity of about $70 − 100$ Gbps and it is estimated that next generation satellites will require capacity of one Terabit/s (1000 Gbps) by 2020 [2]. A key challenge to achieve a Terabit/s broadband satellite communication (SatCom) system is the limited spectrum of about 2 GHz available in current Ka-band. Following the traditional trend, this can be tackled by gradually shifting to a higher frequency band whenever the relevant technology is mature enough.

Therefore, an attractive solution for resolving the issue is moving the feeder link from the Ka-band to the Q/V

band (40/50GHz) where larger bandwidths, up to 5 GHz, are available [2]–[4]. Further, this move can free up the whole Ka-band spectrum for the user link. This is a very interesting solution for satellite operators since the feeder link requires almost the same spectrum as the user link but it does not provide any direct revenue. By moving the feeder link to the unused spectrum, satellite operators can use the freed bandwidth for commercial purposes. Moreover, it allows locating the gateways (GW) within the service area minimizing the interference between the feeder link and user link [4]. However, moving the feeder link to Q/V band imposes considerable strain on the link-budget, which is of the order of $15 − 20$ dB or more predominantly due to heavy rain attenuation [3]. The typical Fade Mitigation Technique (FMT) is the uplink power control. However, it can compensate only a few dBs, thereby motivating the use of multiple GWs for transmit diversity to achieve the required availability in excess of 99.9% on the feeder link. Note that, it is preferable to first use FMTs then GW diversity techniques. Typically, FMTs include a fade prediction block and can handle short and small fades. If these techniques can counter the fade while providing the required performance, GW diversity techniques will not be triggered.

The traditional $1 + 1$ diversity scheme, where one GW is supported by another redundant GW, can be an acceptable solution for low/ medium throughput systems. On the other hand, for high capacity satellite systems where tens of GWs are required, it is not efficient to use the traditional approach. A system employing multiple GWs is the recently launched high throughput KA-SAT which illuminates 82 user spot beams served by 10 GWs (8 active plus 2 redundant). This warrants an investigation into design of advanced diversity techniques.

An interesting GW transmit diversity technique is the $N + P$ diversity scheme, which was studied in [2], [5]–[8]. In this scheme, there are N active GWs and P redundant or idle GWs. When one of the active GWs is in outage, switching occurs and traffic of the active GW is rerouted to one of the idle GWs. Smart GW diversity is another technique which was firstly presented in [9] for Ka-band, and has been studied and developed for Q/V band in [6] and [7]. The benefit of this scheme is that all N GWs are active and there is no need for redundant GWs but its disadvantage is that the throughput of users served by GWs sharing the traffic from their affected counterpart will be reduced or each GW should have some spare capacity available in order to support other GWs in case of outage; hence GWs need to be oversized in capacity. Also, some level of intelligence is required in the user terminals. In

this paper, we will focus on the $N + P$ scheme and present our contributions for this scenario.

Most of the works that studied $N + P$ scheme take a high-level approach for the system design without a rigorous mathematical analysis. To the best of our knowledge, the only work that has analysed GW diversity mathematically is [2] where authors derive the availability in a $N + P$ scenario. However, the authors in [2] do not describe if and how such an availability could be achieved. Further, the switching rate, which is an important system parameter, has not been studied in [2]. A high switching rate can lead to severe overheads and instability thereby warranting its further analysis. In [7], the authors used a simple probabilistic model to study the availability improvement induced by $N + P$ scheme. They assumed that either the link is fully available or it is unavailable. The absence of a rigorous analysis taking into account the dynamic rain attenuation characteristics and practical requirements on switching motivate a further study of the multiple GW paradigm for Q/V band applications.

Contributions of this work are:

- Unlike [1], [2] and [10], we undertake outage analysis incorporating a dynamic model for the rain attenuation samples. For this model, we analytically derive the average outage probability expression for $1 + 1$ configuration that is further used in $N + P$ scenario. The analysis highlights the interplay of switching interval and time correlation as well as the impact of these parameters on performance. Effect of other parameters related to the dynamic modelling (like sampling interval) are studied through simulations.
- Towards accommodating for the latencies incurred during the switching process, we resort to the prediction of Signal-to-Noise-Ratio (SNR). In particular, we find the Minimum Mean Square Error (MMSE) predictor of SNR exploiting the dynamic rain fading model and employ the predicted value for switching. We further study the system performance based on the use of predicted values. The results can also be seen as providing insight into the sensitivity of the switching mechanism to errors in channel estimation.
- We present an efficient switching scheme suited for the $N + P$ gateway scenario. Building on the results from $1 + 1$, we derive closed form expressions for the average outage performance and switching probability on the feeder link. These expressions provide critical insights into system sizing. We also extend the average outage probability study to the end-to-end system which can be further used in system performance evaluations.

The remainder of this paper is organised as follows. Section II introduces the channel model which is used in this paper for generating rain attenuation time series. Section III studies the switching strategy for the $1 + 1$ diversity scheme as the building block of the general $N + P$ scheme. In Section IV, the proposed $N + P$ switching scheme is presented and its performance is evaluated analytically in terms of average outage probability and switching rate. Numerical results are presented in Section V. Concluding remarks are provided in

Section VI.

II. SATELLITE FEEDER LINK CHANNEL MODEL

Radiowave propagation on Earth-space links at Q/V band − and in general in millimeter wave frequencies − is impaired by different tropospheric effects [11], [12]:

- Gaseous absorption due to oxygen and water vapour: This effect is almost constant over time and its statistics can be calculated with the help of the model in ITU-R Recommendation P.676 [13].
- Cloud attenuation: This effect is very slowly varying over time (in minutes or hours) and its statistics can be calculated with the help of the model in ITU-R Recommendation P.840 [14].
- Rain attenuation: It varies slowly over time (order of minutes or few seconds) and its statistics can be calculated with the help of the relevant model in ITU-R Recommendation P.618 [15].
- Scintillations: These are very fast variations (order of milliseconds) and their statistics can be calculated with the help of the relevant model in ITU-R Recommendation P.618.

Of the four effects above, the one driving the dynamics of the gateway diversity is rain attenuation, as gases and clouds are too slow and scintillations are too fast to track. Hence, we focus on rain attenuation in the sequel.

The rain attenuation in dB has been traditionally modelled using a log-normal distribution and the same has been validated by many experimental results [16]. The rain attenuation model in [16] further depends on the rainfall rate. Based on these results, the PDF (Probability Density Function) of the rain attenuation, A (in dB), is modelled as a log-normal variable,

$$p_A(A) = \frac{1}{\sqrt{2\pi}\sigma_L A} \exp\left(-\frac{(\ln A - m_L)^2}{2\sigma_L^2}\right), \quad (1)$$

where m_L and σ_L are the long term mean and standard deviation of $\ln A$, respectively. These quantities can be calculated by fitting a log-normal distribution to the empirical distribution included in ITU-R Recommendation P.618.

Since rain attenuation is a time varying process, in order to design a communication system robust to rain attenuation, it is necessary to model the dynamic behaviour of rain. Several time series models to synthesize rain attenuation samples with temporal properties have been proposed [17]. The stochastic model of Maseng−Bakken [18], which was adopted as a new Recommendation by the Study Group 3 of the ITU-R in 2009 [19], has been the most popular one. This model is based on the fact that the rain attenuation in dB can be modeled as a first order Gauss Markov process of the Ornstein-Uhlenbeck type described by the following stochastic differential equation (SDE) [18], [20],

$$\frac{d\,x(t)}{dt} = -\beta x(t) + \sqrt{2\beta}\,n(t). \quad (2)$$

Here, $x(t) = (\ln A(t) - m_L)/\sigma_L$ and β is the parameter that describes the time dependency of the model. The PDF of the process that satisfies (2) is called transitional PDF and the

process satisfying (2) can be described with a transitional PDF [18] having the form,

$$p_A\left(A(n)|A(n-1)\right) =$$
$$\frac{1}{\sqrt{2\pi}\sigma_{\Delta t}A(n)}\exp\left(-\frac{(\ln A(n) - m_{\Delta t})^2}{2\sigma_{\Delta t}^2}\right), \quad (3)$$

where,

$\sigma_{\Delta t} = \sigma_L\sqrt{1 - \exp\left(-2\beta\Delta t\right)},$
$m_{\Delta t} = m_L[1 - \exp\left(-\beta\Delta t\right)] + \ln A(n-1)\exp\left(-\beta\Delta t\right),$
$\beta = 2 \times 10^{-4}\,\sec^{-1},$

and Δt is the sampling interval of the rain attenuation time series. Equation (3) models the PDF of rain attenuation $A(n)$ at instance $t = n\Delta t$ conditioned on the observation at the previous sampling instance, i.e. $A(n-1)$ at $t_0 = (n-1)\Delta t$.

While the earlier discussion models a single GW to satellite link, the focus of the paper warrants a model for multiple links. Towards this, a n-dimensional generalization was recently proposed in [21] to generate the space-time correlated rain attenuation time series of n links. However, inclusion of spatial correlation makes the analysis intractable and hence we assume spatially independent and identically distributed (i.i.d) links. Further the independence assumption is not unrealistic in the context of a $N + P$ gateway diversity configuration. Typically, if a few tens of gateways are dispersed over Europe, the rain attenuation at their sites tends to be uncorrelated as it takes only few tens of kilometers to achieve decorrelation of rain attenuation. This becomes apparent from applying the correlation coefficient proposed by ITU-R Recommendation P.1815 [22] where the correlation drops to 0.1 at a distance of 90 km. In [1], we studied independent but non-identical GWs case. We located GWs in five European cities (Luxembourg, London, Amsterdam, Berlin and Athens) with different rainfall characteristics. We compared the results with the i.i.d case, where all GWs have the same rainfall characteristics of Luxembourg but fade independently. Numerical results showed that the identical and non-identical cases have a very similar performance. In view of this observation, for the ease of mathematical analysis we use the spatially i.i.d rain attenuation model for further analysis.

III. $1 + 1$ GW CONFIGURATION

A. Switching Strategy

The $1+1$ GW switching scheme is the building block of the general $N + P$ scheme. Hence we first analyze this scheme assuming a dynamic rain attenuation model. We consider a feeder link with an active GW, denoted as G, and an idle GW, denoted as Ḡ. We assume that they are located far away from each other so that they experience independent rain [10]. The GWs sample the beacon signal, assumed to be in the appropriate frequency, every Δt seconds. The channel between the gateways and the satellite at $t = n\Delta t$ is denoted by $h_{i,n} = |h_{i,n}|e^{j\alpha_{i,n}}$ where $\alpha_{i,n} \in (0, 2\pi]$ is the uniformly distributed phase component[1] and $i \in \{1, 2\}$ ($i = 1$ for active

GW and $i = 2$ for idle GW). The channel amplitudes, $|h_{i,n}|$, can be estimated at each GW using a beacon signal received from the satellite. In practice, the beacons measure the total atmospheric attenuation. However, since the gaseous and cloud components are assumed to vary slowly compared to the rain attenuation, their bearing on the decision to switch gateways can be accounted by using a fixed (statistical) margin [2]. Note that, the scintillations are too fast to track, so no attempt is made in the prediction of these fast variations. Thus by measuring the beacon, the decision to switch gateway stations is made in relative terms based on an initial calibration of the beacon signal at each gateway. This is common practice in all operational satellite systems. Motivated by this, we incorporate the simplifying assumption that $|h_{i,n}|$ denotes rain attenuation. As mentioned earlier, the variations in rain attenuation are slow; hence, it is possible to track them and estimate $|h_{i,n}|$ fairly accurately. Since the focus is on the feeder link, the GW exhibits a high clear-sky SNR due to large antenna/ high power amplifier. These arguments corroborate the assumption of an ideal estimation of the channel amplitude in the ensuing analysis. Therefore, the corresponding SNR for the active and idle GWs at $t = n\Delta t$ can be obtained as $\gamma_i(n) = |h_{i,n}|^2\gamma_{CS}$ where γ_{CS} is the clear-sky SNR for the feeder uplink. Thus the measurements can be equivalently seen as providing SNR estimates. The rain attenuation and the channel gains are related as $A_i(n) = -20\log_{10}|h_{i,n}|$.

In our work, the other clear-sky effects are assumed to be compensated by a fixed fade margin or an uplink power control scheme. For tractability of the analysis, we assume identical rain attenuation statistics among the different GWs. Under these assumptions, the corresponding rain attenuations $A_1(n)$ and $A_2(n)$ are i.i.d random variables.

We assume that the GWs are connected to a Network Control Centre (NCC) node which has access to the channel state information of the GWs so that it can estimate $\gamma_1(n)$ and $\gamma_2(n)$ every Δt seconds based on the beacon signal from the satellite. We use two realizations of the time series synthesizer (one per GW) using ITU-R P.1853 [19] summarized in the Section II. Note that, these two series are spatially i.i.d but each exhibits a temporal autocorrelation based on the transitional PDF given in (3). After SNR estimation, the NCC investigates the necessity of switching at intervals of T_{sw} based on the obtained SNR measurements. For ease of implementation, we assume that $T_{sw} = n_{sw}\Delta t$, where n_{sw} is the number of beacon (SNR) samples that NCC uses to perform the GW switching. Fig. 1 illustrates the switching and beacon sample intervals. In general, evaluating the outage performance of the system for the dynamic rain attenuation model is not mathematically tractable. Therefore we first analytically study the outage performance for the special case of $n_{sw} = 1$ or $T_{sw} = \Delta t$, and subsequently attempt the general case of $n_{sw} > 1$. A

---

[1]The phase component is time varying and random due to the imperfections of on-ground and on-board Local Oscillators as well as due to the satellite movement within its station keeping box.

[2]It is a standard engineering task to derive the rain attenuation from the measured beacon value with some margin of error. This error margin will vary depending on the auxiliary equipment used on the gateway site. For example, if the gateway is equipped with a radiometer, cloud attenuation can be estimated with high accuracy and be removed from the total attenuation. Further, if the gateway is equipped with a rain gauge, it may improve the deduction of rain attenuation from total attenuation. For the gaseous contribution, a fixed value will be removed from the total attenuation.
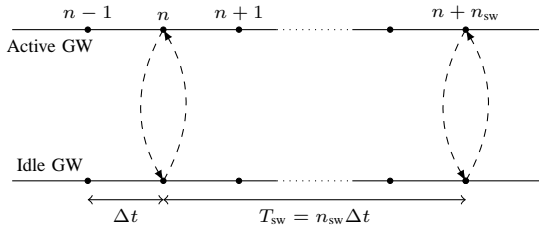
Fig. 1.   Switching intervals in $1 + 1$ Configuration

numerical evaluation illustrating the effect of setting different n_{sw} is presented in Section V.

B. Average Outage Probability for $1+1$ Scheme ($n_{sw} = 1$)

The objective of the study is to analyze the outage performance of the considered multiple GW scheme. The outage enumeration is related to the underlying switching scheme and in this work, we consider the MSSC (modified switch and stay combining) scheme proposed in [10]. According to this scheme, when $T_{\mathrm{sw}} = \Delta t$, the NCC investigates the necessity of switching every Δt and undertakes switching only if SNR of the active GW is below the threshold (γ_{th}) and that the SNR of the idle GW is above the threshold. Denoting the index of the active GW at $t = n\Delta t$ as $\mathcal{A}_n$ and its SNR as $\gamma(n)$, the MSSC is described as,

$$\mathcal{A}_n = 1 \Longleftrightarrow \begin{cases} \mathcal{A}_{n-1} = 1, \gamma_1(n) \geq \gamma_{\mathrm{th}} \\ \mathcal{A}_{n-1} = 1, \gamma_1(n) < \gamma_{\mathrm{th}}, \gamma_2(n) < \gamma_{\mathrm{th}} \\ \mathcal{A}_{n-1} = 2, \gamma_2(n) < \gamma_{\mathrm{th}}, \gamma_1(n) \geq \gamma_{\mathrm{th}} \end{cases} \quad (4)$$

Further, $\mathcal{A}_n = 2$ can be obtained similarly.

To exploit the temporal correlation, we exploit the fact that the NCC knows the attenuation from all the GWs at time instances $\{(n-k)\triangle t\}_{k \geq 1}$. Further, the NCC also knows the GW active at instances $\{(n-k)\triangle t\}_{k \geq 1}$. The instantaneous outage probability at $t = n\Delta t$ exploiting time correlation then takes the generic form, $\Pr\{\gamma(n) \leq \gamma_{\mathrm{th}} | \{\gamma_1(n-k), \gamma_2(n-k), \mathcal{A}_{n-k}\}_{k \geq 1}\}$. Using the fact that rain attenuation is a first-order Markov [18], the aforementioned expression reduces to $\Pr\{\gamma(n) \leq \gamma_{\mathrm{th}} | \gamma_1(n-1), \gamma_2(n-1), \mathcal{A}_{n-1}\}$. Since $\gamma_k(n-1)$ are random variables, so is, $\Pr\{\gamma(n) \leq \gamma_{\mathrm{th}} | \gamma_1(n-1), \gamma_2(n-1), \mathcal{A}_{n-1}\}$ and towards defining a statistical measure of outage at $t = n\Delta t$, we define,

$$P_n = \mathrm{E}\left[\Pr\{\gamma(n) \leq \gamma_{\mathrm{th}} | \gamma_1(n-1), \gamma_2(n-1), \mathcal{A}_{n-1}\}\right], \quad (5)$$

where $\mathrm{E}(\cdot)$ is the expectation operation over $\{\gamma_k(n-1)\}$ and $\mathcal{A}_{n-1}$. Note that, the PDF of $\gamma_k(n-1)$ (in dB) can be obtained from (1) and that we assume $\mathcal{A}_{n-1}$ takes values $\{1, 2\}$ equally likely. The last assumption follows from the identical distribution of the rain attenuation across the two GWs. While P_n is no longer a random variable, it is time varying. The time variations are further averaged to yield the *average outage probability* of $1 + 1$ scheme as,

$$\bar{P}_{1+1}(\gamma_{\mathrm{th}}) = \frac{1}{N_r} \sum_{n=1}^{N_r} P_n \ . \quad (6)$$

where N_r is the number of samples in the time series.

The discussion so far has been agnostic to the switching strategy. We now incorporate the MSSC strategy for further simplification. Specializing to the case of $\mathcal{A}_{n-1} = 1$ and employing (4), we have,

$$\Pr\{\gamma_n \leq \gamma_{\mathrm{th}} | \gamma_1(n-1), \gamma_2(n-1), \mathcal{A}_{n-1} = 1\}$$
$$= \Pr\{\gamma_1(n) \leq \gamma_{\mathrm{th}}, \ \gamma_2(n) \leq \gamma_{\mathrm{th}} | \gamma_1(n-1), \gamma_2(n-1)\}, \quad (7)$$

wherein we exploit the first order Markov property of rain attenuation [18] and the fact that the first GW was active at the instance $n-1$. Using the spatial independence of the rain attenuations, (7) can be simplified as,

$$\Pr\{\gamma_1(n) \leq \gamma_{\mathrm{th}}, \ \gamma_2(n) \leq \gamma_{\mathrm{th}} | \gamma_1(n-1), \gamma_2(n-1)\} \quad (8)$$
$$= \Pr\{\gamma_1(n) \leq \gamma_{\mathrm{th}} | \gamma_1(n-1)\} \Pr\{\gamma_2(n) \leq \gamma_{\mathrm{th}} | \gamma_2(n-1)\}.$$

Using the relation between the rain attenuation and the SNR, we further simplify (8) as,

$$\Pr\{\gamma_1(n) \leq \gamma_{\mathrm{th}}, \ \gamma_2(n) \leq \gamma_{\mathrm{th}} | \gamma_1(n-1), \gamma_2(n-1)\} \quad (9)$$
$$= \Pr\{A_1(n) > \alpha_{\mathrm{th}} | A_1(n-1)\} \Pr\{A_2(n) > \alpha_{\mathrm{th}} | A_2(n-1)\},$$

where $\alpha_{\mathrm{th}} = 10 \log(\gamma_{CS}/\gamma_{\mathrm{th}})$. Further, a similar result holds when $\mathcal{A}_{n-1} = 2$. Using the identical distribution of the $A_k(n), k = 1, 2$ and equally like occurrence of $\mathcal{A}_{n-1} = 1, 2$, it is shown in Appendix A, that

$$P_n = \frac{1}{4} \operatorname{erfc}\left(\frac{\ln \alpha_{\mathrm{th}} - m_L}{\sqrt{2}\sigma_L}\right)^2. \quad (10)$$

Using (10), the average outage probability can be finally written as

$$\bar{P}_{1+1}(\gamma_{\mathrm{th}}) = \frac{1}{4} \operatorname{erfc}\left(\frac{\ln \alpha_{\mathrm{th}} - m_L}{\sqrt{2}\sigma_L}\right)^2. \quad (11)$$

Remark 1: Effect of Time Correlation: The average outage probability in (11) is independent of Δt. In fact, (11) can be easily deduced as the outage probability when considering time-independent rain attenuation samples [10]. One could argue that the use of the current SNR sample for switching invalidates the introduction of the time correlation. However, the outage probability expressions are derived for MSSC which implicitly exploits time correlation. This non-appearance of the time correlation is made possible because the outage threshold in (9) is independent of $A_k(n-1)$ unlike, for example, derivations involving the evaluation of Bit Error Rates for fading channels. However, it should be stressed that, unlike the temporally independent scenario, $\bar{P}_{1+1}(\gamma_{\mathrm{th}}) \neq \Pr\{\gamma(n) \leq \gamma_{\mathrm{th}} | \gamma_1(n-1), \gamma_2(n-1), \mathcal{A}_{n-1}\}$ when the dynamic model is exploited. The observation implies that the correlation between rain samples, as dictated by (3), can have favorable as well as adverse effects.

C. Average Outage Probability for $1+1$ Scheme ($n_{sw} > 1$)

We now study the outage probability for the $1 + 1$ configuration when $n_{\mathrm{sw}} > 1$. This assumes a random switching interval, T_{sw}, that includes n_{sw} SNR samples. In such a scenario, it is natural to include the number of outages in addition to their occurrence. Hence, we extend the definition of (5) to $P_k =$

$\frac{1}{n_{\text{sw}}} \left[\text{E}\{ \Pr\{ \gamma(k) < \gamma_{\text{th}} | \{\gamma_m(k-1)\}_m, \mathcal{A}_{k-1} \} \} + \text{E}\left[n_{\text{out}}(k) \right] \right]$, where $n_{\text{out}}(k)$ is the number of SNR samples (measured at the active GW) that are in outage during the interval $[k + 1, k + n_{\text{sw}} - 1]$ and the expectation is over $\{\gamma_m(k-1)\}_m, \mathcal{A}_{k-1}$. While the first term provides the outage at the switching instance, $\text{E}\left[n_{\text{out}}(k) \right]$ results in the average number of outages in the remaining $n_{\text{sw}} - 1$ samples. Thus the measure gives the notion of probability and reduces to (5) when $n_{\text{sw}} = 1$.

Further, $\text{E}\{n_{\text{out}}(k)\}$ can be expressed as,

$$\text{E}\left[n_{\text{out}}(k) \right] = \sum_{l=1}^{n_{\text{sw}}-1} l \, \text{E}\left[\Pr\{ n_{\text{out}}(k) = l \, | \gamma(k-1) \} \right]. \quad (12)$$

Evaluation of each of the terms in (12) involves correlated rain samples, thereby making it involved if not untractable. In the following, we illustrate with an example that not all terms are independent of $\beta \Delta t$ as in the case of $n_{\text{sw}} = 1$.

Example: Consider $n_{\text{sw}} = 3$ and we consider $n_{\text{out}} = 2$. It can be shown that

$$\text{E}\left[\Pr\{ n_{\text{out}} = 2 \, | \gamma_{k-1} \} \right] = \quad (13)$$
$$\int_0^{\gamma_{th}} \int_0^{\gamma_{th}} f\left(x, y; (m_L, \sigma_L^2), (m_L, \sigma_L^2), e^{-\beta \Delta t} \right) \, dx \, dy$$

where $f\left(x, y; (m_L, \sigma_L^2), (m_L, \sigma_L^2), e^{-\beta \Delta t} \right)$ is the bi-variate log-normal distribution with the variables x, y having m_L as mean, σ_L as variance and $e^{-\beta \Delta t}$ as the correlation [23].

Remark 2: A key observation is that P_k has components that are no longer independent of $\beta \Delta t$. While it is difficult to characterize their effect analytically, the effects of the dynamic model are further discussed in Section V where their effects are illustrated through numerical evaluations.

While we have derived the expression for $n_{\text{sw}} = 2$, a similar exercise for $n_{\text{sw}} > 2$ becomes rather involved. However, we can find an approximate expression by assuming the SNR samples to be i.i.d spatially and temporally. In this case, it can be written as $\sum_{i=0}^{n_{\text{sw}}-1} i \binom{n_{\text{sw}}-1}{i} p^i (1-p)^{n_{\text{sw}}-1-i}$, where $p = \Pr\{\gamma(k) < \gamma_{\text{th}}\} = \frac{1}{2} \text{erfc}\left(\frac{\ln \alpha_{\text{th}} - m_L}{\sqrt{2}\sigma_L} \right), \forall k$, $kn_{\text{sw}} + 1 \leq j < (k+1)n_{\text{sw}}$, wherein we exploit the identical distribution of attenuation samples for all GWs. The average outage probability, $\bar{P}_{1+1}$, can be approximated by,

$$\bar{P}_{1+1} \approx \frac{p^2 + (n_{\text{sw}} - 1)p}{n_{\text{sw}}}. \quad (14)$$

When $n_{\text{sw}} = 1$ (14) reduces to (11). Further, if $n_{\text{sw}} = 1$, average outage probability will be p^2 regardless of the correlation between the sample (as it was shown for correlated samples in subsection III-A) and it naturally means that we will get the best performance when switching is checked for every sample. If $n_{\text{sw}} \to \infty$, we will have $\bar{P}_{1+1} = p$. This means that if the time interval between switching instances is too long, the system will not benefit from the second GW since its performance is equal to the single GW system. Numerical simulations corroborating this observation is presented in Section V.

D. Switching Based on SNR Prediction

In practice, the switching operation is not instantaneous and there is a latency between making the decision and executing it. This implies that actual switching is effected only at $t + t_d$ if the decision to switch is made at t. However, the value of the SNRs at the actual switching instance would be different from those resulting in the decision. One way to solve this problem is to predict the rain attenuation t_d seconds ahead, derive the corresponding SNR and make a decision based on these predicted values.

There are different methods for the fade predicting depending on the model assumed for the channel, see [24]–[26]. For the channel model assumed in this paper, we can exploit (3) to derive the MMSE estimator which is used to estimate the $A(t + t_d)$ based on the observed $A(t)$. It is known that the MMSE estimator is the mean of the posterior PDF [27]. The posterior PDF of $A(t + t_d)$ given the observation $A(t)$ can be obtained by (3) and the MMSE estimate as follows,

$$\hat{A}(t + t_d) = \exp\left(m_{t_d} + \sigma_{t_d}^2/2 \right), \quad (15)$$

where m_{t_d} and σ_{t_d} similar to (3) with Δt replaced by t_d. During the switching interval (time duration between making the decision and executing it) we assume that the active GW continues serving the users until switching is effected.

While the instantaneous estimation of the channel using beacon is assumed to be ideal, errors would be induced by the prediction. Use of predicted values can be seen as a representative case towards evaluating the performance of the system with decision errors and indicative of its sensitivity to imperfect channel information. Further the quality of the estimate is indicative of the correlation and hence switching based on prediction reflects the influence of time correlation as well. Clearly, increasing t_d reduces correlation and enhances prediction errors; Section V will discuss the effect of t_d on the performance of the system.

IV. $N + P$ GW CONFIGURATION

In this section, we consider a generalized switching scheme with N active GWs and P idle GWs. Similar to the 1+1 analysis, we continue the use of the dynamic rain fading model for every link, while assuming the links themselves to be spatially i.i.d. The latter assumption, used for mathematical tractability, is motivated in Section II and implies that all GWs have the same rain attenuation statistics and are independent. We have dropped n (time sample index) from the expressions for simplicity. Based on the MSSC strategy in Section III-A, a switching scheme for $N + P$ scenario is presented first (see also [1]), followed by an analysis of the outage probability as well as switching rate.

A. $N + P$ GW Switching Strategy

Fig. 2 illustrates the switching strategy in detail and the different steps are explained in detail below.

- **Acquisition**: In the first step, NCC collects the SNR of all GWs, both active and idle.
- **Sorting**: After acquisition, the NCC sorts the active and idle GWs based on their SNR in *decreasing* order (this is
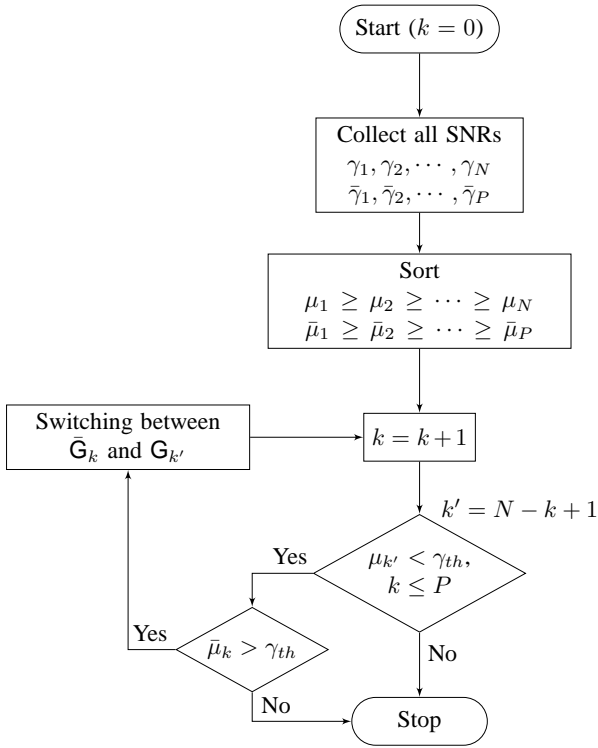
Fig. 2.   Flowchart of $N + P$ Gateway Switching scheme

same as sorting the GWs based on their rain attenuation in *increasing* order). The mth largest SNR amongst the active GWs and the corresponding GW index are denoted by μ_m and G_m, respectively. Similarly, for the idle GWs, the kth largest SNR and the corresponding GW index are depicted by $\bar{\mu}_k$ and $\bar{\mathsf{G}}_k$, respectively. Therefore, we can write $\mu_1 \geq \mu_2... \geq \mu_N$ and $\bar{\mu}_1 \geq \bar{\mu}_2 \cdots \geq \bar{\mu}_P$. Defining A_i and $\bar{A}_i$ to be the rain attenuation of G_i and $\bar{\mathsf{G}}_i$, respectively, we obtain $A_1 \leq A_2 \leq \cdots \leq A_N$ and $\bar{A}_1 \leq \bar{A}_2 \leq \cdots \leq \bar{A}_P$ by exploiting the relation between the channel gain and rain attenuation.

- **Pairing**: After the sorting step, NCC initiates pairing the active $\mathsf{G}_{k'}$ and idle $\bar{\mathsf{G}}_k$ GWs, where $k = 1,...,P$ and $k' = N - k + 1$. Thus, P switching pairs will be formed such that the weakest active GW, G_N, will have the best chance to switch to the strongest idle GW, $\bar{\mathsf{G}}_1$.

- **Switching**: The switching between the pairs will take place based on MSSC scheme introduced for two GWs in [10]. Based on this switching method, if $\mu_{k'}$ is lower than γ_{th} and $\bar{\mu}_k$ is higher than γ_{th}, switching occurs between two GWs. Here, γ_{th} is the outage threshold.

Note that, in each time slot, the state of the GWs (active or idle) can change due to switching. However, this will not impact the ensuing statistical analysis since the SNR associated with different GWs have independent and identical distribution.

Complexity: Regarding the complexity of the switching algorithm, it should be noted that the switching process involves the sorting and comparison operations where sorting operation has a complexity of $\mathcal{O}(n \log n)$ in worst case [28].

It is assumed that the NCC handles traffic rerouting when a decision to switch is undertaken. This process could involve higher layers which could have a bearing on the performance. For example, packet-loss during the switching process is an issue studied in [8]. The analysis of such issues is pertinent; however, the current work focuses on analyzing physical layer performance and higher layer issues like traffic rerouting (switching) are left for further investigation. As such, our contribution should be construed as only a building block that needs to be combined with other higher layer tools for carrying out cross-layer system optimization.

B. Average Outage Probability

In this subsection, we will study the performance of the proposed $N+P$ scheme for the feeder link in terms of average outage probability when switching is considered for every sample. We define the $N + P$ average outage probability of the feeder link as,

$$\bar{P}_{FL}(\gamma_{\text{th}}) = \frac{1}{N} \left(\sum_{m=1}^{N-P} \bar{Q}_m + \sum_{k=1}^{P} \bar{P}_{1+1,k} \right). \qquad (16)$$

Here $\bar{Q}_m, 1 \leq m \leq N-P$, is the average outage probability of each of the $N - P$ GWs that are not involved in the switching process. Further, $\bar{P}_{1+1,k}$ [3] is the average outage probability of kth pair from the P switching pairs.

We now evaluate $\bar{P}_{1+1,k}$ and $\bar{Q}_m$. The methodology used in Section III-B is applicable to the current scenario in a straight forward manner, but with additional book keeping. Omitting the additional details for ease of comprehension, the average outage probabilities of the switching pairs, $\mathsf{G}_{k'}$ and $\bar{\mathsf{G}}_k$, can be calculated as,

$$\begin{aligned} \bar{P}_{1+1,k}(\gamma_{\text{th}}) &= \Pr\{\mu_{k'} \leq \gamma_{\text{th}}\} \Pr\{\bar{\mu}_k \leq \gamma_{\text{th}}\} \\ &= \Pr\{A_{k'} > \alpha_{\text{th}}\} \Pr\{\bar{A}_k > \alpha_{\text{th}}\} \\ &= \left(1 - P_{A_{k'}}(\alpha_{\text{th}})\right) \left(1 - P_{\bar{A}_k}(\alpha_{\text{th}})\right) \end{aligned} \qquad (17)$$

The outage probability of the remaining $N - P$ active GWs, that are not involved in the switching process can be calculated as

$$\bar{Q}_m(\gamma_{\text{th}}) = \Pr\{\mu_m \leq \gamma_{\text{th}}\} = 1 - P_{A_m}(\alpha_{\text{th}}). \qquad (18)$$

In (17) and (18), $P_{A_m}(\cdot)$ and $P_{\bar{A}_k}(\cdot)$ are the Cumulative Distribution Function (CDF) of mth and kth order statistics of A and $\bar{A}$, respectively. These CDFs can be obtained from [29] as,

$$P_{A_{k'}}(\alpha_{\text{th}}) = \sum_{t=k'}^{N} \binom{N}{t} \left[P_A(\alpha_{\text{th}})\right]^t \left(1 - P_A(\alpha_{\text{th}})\right)^{N-t}, \quad (19)$$

$$P_{A_k}(\alpha_{\text{th}}) = \sum_{t=k}^{P} \binom{P}{t} \left[P_A(\alpha_{\text{th}})\right]^t \left(1 - P_A(\alpha_{\text{th}})\right)^{P-t}. \quad (20)$$

---

[3] We slightly abuse the notation $\bar{P}_{1+1}$ of (6) to incorporate the kth pair; each pair employs ordered SNR and hence the average outage probability would be different.

Towards obtaining (16), it now remains to evaluate $P_A(\alpha_{\text{th}})$. Since rain attenuation follows the log-normal distribution in (1), $P_A(\alpha_{\text{th}})$ can be obtained as,

$$P_A(\alpha_{\text{th}}) = 1 - 0.5 \operatorname{erfc}\left(\frac{\ln \alpha_{\text{th}} - m_L}{\sqrt{2}\sigma_L}\right). \qquad (21)$$

Finally, by substituting (17) and (18) in (16), we get an expression for the feeder link average outage probability of the system as,

$$\bar{P}_{FL}(\gamma_{\text{th}}) = \frac{1}{N} \sum_{m=1}^{N-P} \left(1 - P_{A_m}(\alpha_{\text{th}})\right) \qquad (22)$$
$$+ \frac{1}{N} \sum_{k=1}^{P} \left(1 - P_{A_{k'}}(\alpha_{\text{th}})\right) \left(1 - P_{\bar{A}_k}(\alpha_{\text{th}})\right).$$

To illustrate the generalization of the derived expressions, it can be easily shown that the result in (11) can be obtained from (22) by using $N = P = 1$. Note that, similar to the expression in (11), equation (22) will be independent of the temporal correlation when $n_{\text{sw}} = 1$. It should be noted that (22) is similar to the result of [2]; however, the current work employs a bottom-up approach where the switching strategy is defined and the resulting outage is then calculated.

Remark 3: While the earlier discussion focused on $n_{\text{sw}} = 1$, the ideas of Section III-C on $n_{\text{sw}} > 1$ can be extended to the $N + P$ configuration. Fortunately, the computation of $\mathrm{E}\left[n_{\text{out}}(k)\right]$ does not involve ordered SNRs.

C. End-to-End Outage Analysis

Given that the user link (link between the satellite and user) will operate in a band (like Ka) lower than the feeder link, it is interesting to investigate the improvement of the end-to-end link due to $N + P$ scheme. The vast majority of SatCom systems are transparent − the satellite repeater only downconverts the signal received on the feeder link and amplifies it before re-transmitting onto the user link.

To study the end-to-end performance of the system, we assume that each active GW serves a single user in each time slot considering time division multiple access (TDMA) channel. Therefore, we can assume that there are N end-to-end links (GW to the user terminal). The average outage probability of $N + P$ scheme will be the average of these N end-to-end links.

Following a similar approach used in (12) of [10], we can find the outage probability of the lth end-to-end link as,

$$\bar{P}_{E2E,l}(\gamma_{\text{th}}) = \bar{P}_{FL,l}(\gamma_{\text{th}}) + \int_{\gamma_{\text{th}}}^{\infty} \bar{P}_{FL,l}(z) f_{\gamma_g}(\gamma_g) d\gamma_g \qquad (23)$$

where $z = \gamma_{\text{th}}(\gamma_g + 1)/(\gamma_g - \gamma_{\text{th}})$ and $1 \le l \le N$. γ_g is the SNR of a Ka-band user link which is assumed to have a log-normal PDF ($f_{\gamma_g}(\cdot)$) and $\bar{P}_{FL,l}(\cdot)$ is the outage probability of the feeder link in each of the N end-to-end links. For the active GWs involved in the switching process, $\bar{P}_{FL,l}(\cdot)$ can be found using (17) and for those not involved in the switching process it can be found from (18).

Therefore, average end-to-end outage performance of a transparent satellite with $N + P$ GWs can be found as,

$$\bar{P}_{E2E}(\gamma_{\text{th}}) = \frac{1}{N} \sum_{l=1}^{N} \bar{P}_{E2E,l}(\gamma_{\text{th}})$$
$$= \bar{P}_{FL}(\gamma_{\text{th}}) + \int_{\gamma_{\text{th}}}^{\infty} \bar{P}_{FL}(z) f_{\gamma_g}(\gamma_g) d\gamma_g \qquad (24)$$

where $\bar{P}_{FL}(\gamma_{\text{th}})$ is defined in (22). Here, we assumed that SNRs of all user links are i.i.d with the same PDF, $f_{\gamma_g}(.)$.

D. Average Switching Rate

When GW switching is used, the switching rate is an important issue since a high switching rate results in large overhead and can make the system unstable. Let the number of switching instances be denoted by N_{sw} and the total number of the SNR (rain attenuation) samples by N_r. We also assume that the investigation for switching is done for every sample, e. g. $T_{\text{sw}} = \Delta t$ since $n_{\text{sw}} = 1$. Then, the switching probability can be expressed as $\frac{N_{\text{sw}}}{N_r}$ and switching rate as *Switching Probability* $/\Delta t$. Note that, the switching rate is actually defined as the ratio of number of switching instances over the total time, e.g. $N_{\text{sw}}/(N_r \Delta t)$. For a fixed value of N_r and based on this definition, the lower the time interval between the samples (Δt), the lower will be the switching probability. This is because, for small values of Δt, the rain attenuation samples are highly correlated. As Δt increases, correlation between the samples decreases and results in a higher switching probability.

In this subsection, for the ease of mathematical analysis, we consider the i.i.d samples (large Δt) which leads to the upper bound of the switching probability. In Section V, we will study the effect of different Δt on the switching probability by numerical simulation.

As explained in Section IV, switching will occur between $\mu_{k'}$ and $\bar{\mu}_k$ based on MSSC scheme. Hence, similar to the approach used in [10] for i.i.d random variables, it is possible to define a six state Markov chain model for each switching pair. The transitional probability matrix $\mathbf{P}$ of the Markov chain can be obtained as (for details kindly refer to [10]),

$$\mathbf{P} = \begin{pmatrix} \rho_{k'} & p_k & 1 - \rho_{k'} - p_k & 0 & 0 & 0 \\ \rho_{k'} & p_k & 1 - \rho_{k'} - p_k & 0 & 0 & 0 \\ 0 & 0 & 0 & \varrho_k & p_k & 1 - \varrho_k - p_k \\ 0 & 0 & 0 & \varrho_k & p_k & 1 - \varrho_k - p_k \\ 0 & 0 & 0 & \varrho_k & p_k & 1 - \varrho_k - p_k \\ \rho_{k'} & p_k & 1 - \rho_{k'} - p_k & 0 & 0 & 0 \end{pmatrix}, \qquad (25)$$

where $\rho_{k'} = P_{A_{k'}}(\gamma_{\text{th}})$, $p_k = (1 - P_{A_{k'}}(\gamma_{\text{th}}))(1 - P_{A_k}(\gamma_{\text{th}}))$ and $\varrho_k = P_{\bar{A}_k}(\gamma_{\text{th}})$. We define $\pi_{i,k}$ as the probability that kth switching pair is in state i. By using the facts that $\overrightarrow{\pi} = \overrightarrow{\pi}\mathbf{P}$ and $\sum_{i=1}^{6} \pi_{i,k} = 1$, where $\overrightarrow{\pi} = [\pi_{1,k}, \pi_{2,k}, ..., \pi_{6,k}]$, the switching probability of kth pair can be calculated as

$$\pi_k(\gamma_{\text{th}}) = \frac{2(1 - \rho_{k'} - p_k)(1 - \varrho_k - p_k)}{2 - \rho_{k'} - \varrho_k - 2p_k}, \qquad (26)$$

Now, we can define the average switching probability as

$$P_{\text{sw}} = \frac{1}{P} \sum_{k=1}^{P} \pi_k(\gamma_{\text{th}}). \qquad (27)$$

TABLE I
PROPAGATION AND LINK BUDGET ASSUMPTIONS

Q/V band Feeder Up-Link	Value
Carrier frequency	50 GHz
Elevation angle	32°
Polarization	Circular
$EIRP_{GW}$ including back-off	76.5 dBW
UL free space loss	218.3 dB
$(G/T)_{Sat}$	31.45 dB
γ_{CS}	28.3 dB

TABLE II
PROPAGATION AND LINK BUDGET ASSUMPTIONS

Ka-band User Down-Link	Value
Carrier frequency	20 GHz
Elevation angle	35°
Polarization	Circular
$EIRP_{sat}$ including back-off	72.5 dBW
DL free space loss	210.5 dB
$(G/T)_{UT}$	20.3 dB
γ_{CS}	21.3 dB
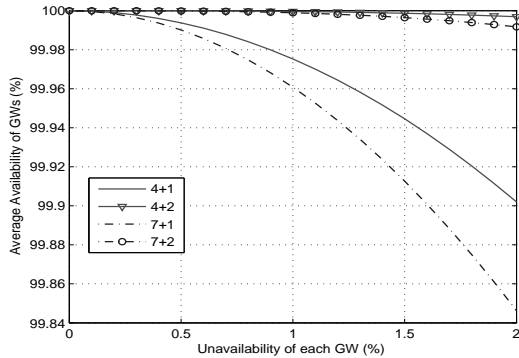
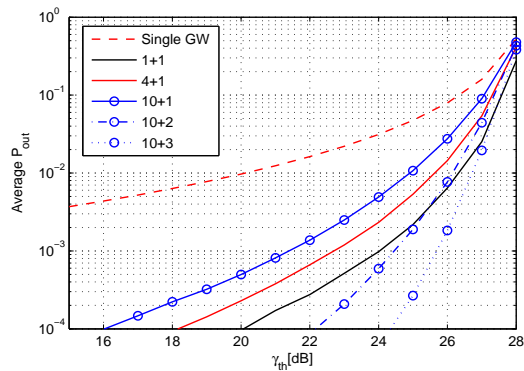Fig. 3. Average availability of the GWs versus unavailability of a single GW

Fig. 4. Average outage probability for different $N + P$ configurations

The switching rate can be easily calculated as $P_{sw}/\Delta t$ where Δt is the interval between switching instants. In Section V, we will see that how Δt affects the switching rate.
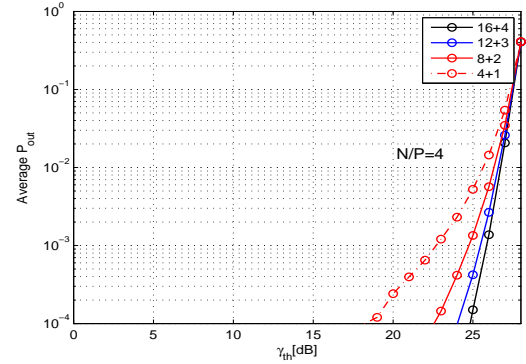

Fig. 5. Average outage probability for $\frac{N}{P} = 4$ and different $N + P$ schemes
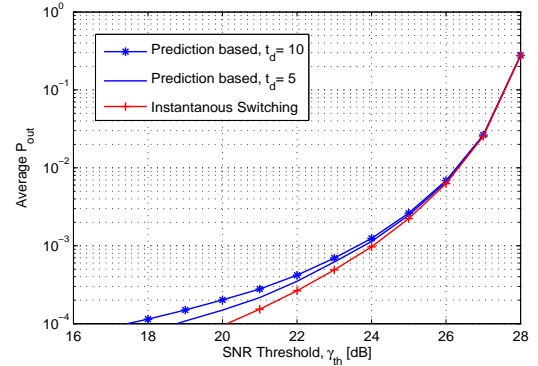

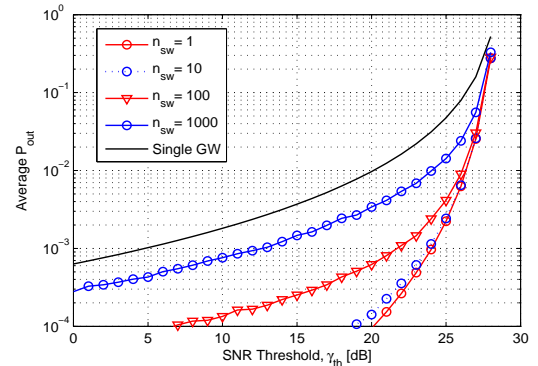Fig. 6. Average outage probability of $1 + 1$ case for different estimation lags and $\Delta t = 1$

Fig. 7. Feeder Link average outage probability of $1 + 1$ case for different n_{sw} and $\Delta t = 1$

V. NUMERICAL RESULTS AND DISCUSSION

Tables I and II respectively detail the propagation parameters and the link budget parameters for typical Central-European climate that were used as input to the empirical rain attenuation prediction model included in ITU-R Recommendation P.618. For simulation purposes, we consider a dynamic rain attenuation model based on [19] wherever Δt is used. In this method, rain attenuation samples are synthesized from a discrete white Gaussian noise process. In the first step, the white Gaussian noise is low-pass filtered and then transformed from a normal distribution to a log-normal distribution. Finally,
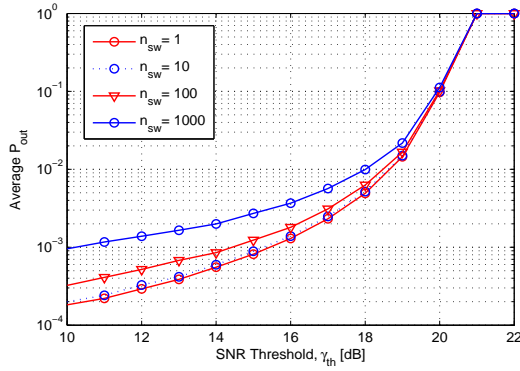
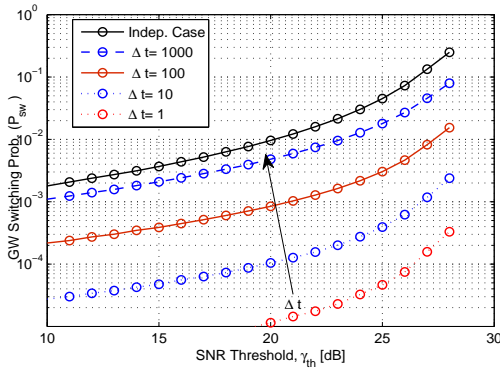Fig. 8. End-to-end average outage probability of $1+1$ case for different n_{sw} and $\Delta t = 1$

Fig. 9. GW Switching Probability for $1+1$ scheme and different Δt and $n_{\mathrm{sw}} = 1$
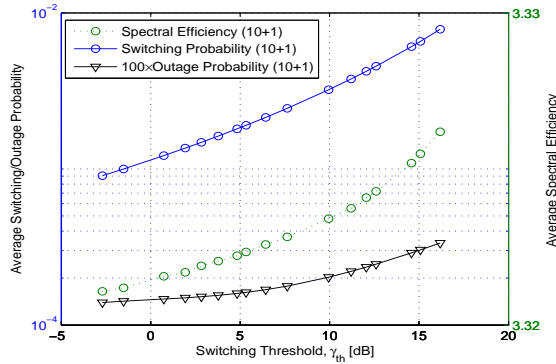

Fig. 10. Average Switching probability and Spectral Efficiency for different switching thresholds

it is calibrated to match the desired rain attenuation statistics.

Fig. 3 presents the average availability $(1 - \bar{P}_{FL}$ in percentage) of the large scale GW diversity scheme versus unavailability of a single GW $(1 - P_A(\alpha_{\mathrm{th}})$ in percentage). For the case of $4+1$ and $7+1$, it can be seen that if availability of each GW is 99%, the average availability of the whole GW network will be around 99.97% and 99.96%, respectively. This figure is obtained from (22).

Fig. 4 illustrates the feeder-link outage performance of the proposed scheme for different configurations. It is aimed at providing some insights about the effect of N, P on

performance and aid in system design. We can see that, with the number of idle GWs fixed ($P = 1$), the outage probability degrades gracefully with increasing number of active GWs. This means that if we assign only one idle GW for 10 active GWs, this scheme could still provide acceptable outage performance. Also, it can be seen that for a fixed number of active GWs ($N = 10$), if we increase the number of idle GWs from 1 to 2 outage probability decreases considerably. It is worth mentioning that all results are theoretical evaluations.

Fig. 5 presents the average outage probability of different configurations when $\frac{N}{P} = 4$. It can be inferred from the figure that for a fixed ratio of $\frac{N}{P}$, if the number of GWs increases, the system will have a better outage performance. This means that, for example, if there are 8 active GWs and 2 idle GWs, the $8+2$ architecture will result in better overall performance than two $4+1$ clusters.

Fig. 6 illustrates the performance of the $1+1$ system when switching is done based on the predicted value of the rain attenuation. As it can be seen, increasing t_d degrades the outage performance of the system. For the availability of 99.9% ($\bar{P}_{out} = 10^{-3}$), performing switching based on the prediction results in 0.25 dB and 0.4 dB degradation in the outage performance for $t_d = 5$ seconds and $t_d = 10$ seconds, respectively.

Fig. 7 shows the effect of setting different n_{sw} (recall that n_{sw} is the number of SNR samples between two switching check instances) on the outage probability of the $1+1$ system. In this case, we assume that NCC checks the switching possibility every n_{sw} samples and switching is performed instantaneously. As expected, increasing the n_{sw} degrades the system performance because switching is not done on time to cope with the outages. For the considered operating point of $\bar{P}_{out} = 10^{-3}$, it can be seen that the performance is affected considerably. For very high values of n_{sw}, the performance curve converges to that of the single GW system. In $N + P$ scheme, n_{sw} will have the similar effect. We can derive the similar conclusions from Fig. 8 for the end-to-end average outage probability.

Fig. 9 presents the switching probability of the $1+1$ scheme for different Δt. As it was discussed in subsection IV-D, larger Δt increases the switching probability. It can be seen that as $\Delta t \to \infty$, switching probability converges to the upper bound described by (27).

Fig. 10 shows the influence of different switching thresholds on the switching probability, average outage probability and the spectral efficiency of the system. In fact, γ_{th} is chosen correspond to the minimum SNR required to support a certain Modcod in DVB-S2. It can be seen that the improvements in spectral efficiency are negligible while the switching rate is sensitive to the threshold. As expected, by increasing γ_{th}, the switching probability of the system increases and so does the spectral efficiency.

VI. CONCLUSION

In this paper, we have devised a practical switching scheme to exploit multiple GW transmit diversity when moving the feeder link of a multibeam broadband satellite network to

Q/V band. The novel aspect of the proposed scheme are the association of GWs into switching pairs based on ordered SNR and the use of the robust MSSC strategy. Also, considering a dynamic rain attenuation model, we have studied the effect of performing switching based on the predicted rain attenuation values. Expressions for key performance indicators − average outage probability and switching rate− have been derived analytically providing insights into system sizing especially on the relative effect of the number of idle and active GWs. An interesting result is that larger clusters yield better performance for a given ratio of idle and active GWs. It is further seen that an increase in switching threshold, enhances achieved spectral efficiency, but at the cost of higher switching probability.

APPENDIX A
PROOF OF THE EQ. (10)

Proof: Since $A_1(n-1)$ and $A_2(n-1)$ are independent, the expression of interest reduces to

$$P_n = \frac{1}{4} \, \mathrm{E} \left\{ P\{A_1(n) > \alpha_{\text{th}} | A_1(n-1)\}\right\}$$
$$\mathrm{E} \left\{ P\{A_2(n) > \alpha_{\text{th}} | A_2(n-1)\}\right\}. \tag{28}$$

We now evaluate $\mathrm{E} \left\{ P\{A_1(n) > \alpha_{\text{th}} | A_1(n-1)\}\right\}$ and the result in (6) follows due to the spatial i. i. d nature of rain attenuation. For simplicity, we rewrite the expression under evaluation as,

$$\mathrm{E}_y \left[\Pr\{x > \alpha_{\text{th}} | y\} \right] = \mathrm{E}_y \left[\int_{\alpha_{\text{th}}}^{\infty} f(x|y) dx \right]$$
$$= \int_0^{\infty} \int_{\alpha_{\text{th}}}^{\infty} \underbrace{f(x|y) f(y)}_{f(x,y)} \, dx \, dy = \int_{\alpha_{\text{th}}}^{\infty} \int_0^{\infty} f(x,y) \, dy \, dx$$
$$= \int_{\alpha_{\text{th}}}^{\infty} f(x) dx = \Pr\{A_1(n) > \alpha_{\text{th}}\}$$
$$= 0.5 \, \mathrm{erfc} \left(\frac{\ln \alpha_{\text{th}} - m_L}{\sqrt{2}\sigma_L} \right).$$

∎

REFERENCES

[1] A. Gharanjik, B. S. M. R. Rao, P.-D. Arapoglou, and B. Ottersten, "Large scale transmit diversity in Q/V band feeder link with multiple gateways," in *2013 IEEE 24th International Symposium on Personal Indoor and Mobile Radio Communications (PIMRC)*, Sep. 2013, pp. 766–770.

[2] A. Kyrgiazos, B. Evans, P. Thompson, and N. Jeannin, "Gateway diversity scheme for a future broadband satellite system," in *Advanced Satellite Multimedia Systems Conference (ASMS) and 12th Signal Processing for Space Communications Workshop (SPSC), 2012 6th*, 2012, pp. 363–370.

[3] P.-D. Arapoglou, M. R. B. Shankar, A. Panagopoulos, and B. Ottersten, "Gateway diversity strategies in Q/V band feeder links," in *17th Ka and Broadband Communications Conference, Palermo, Italy*, 2011.

[4] O. Vidal, G. Verelst, J. Lacan, E. Alberty, J. Radzik, and M. Bousquet, "Next generation high throughput satellite system," in *IEEE First AESS European Conference on Satellite Telecommunications (ESTEL*, 2012, pp. 1–7.

[5] D. Mignolo, E. Re, A. Ginesi, A. B. Alamanac, P. Angeletti, and M. Harverson, "Approaching terabit/s satellite: a system analysis," in *17th Ka and Broadband Communications Conference*, Palermo, Italy, 2011.

[6] P. Angeletti, R. De Gaudenzi, and E. Re, "Smart gateway diversity," *Patent Description, European Space Agency*, 2012.

[7] N. Jeannin, L. Castanet, J. Radzik, M. Bousquet, B. Evans, and P. Thompson, "Smart gateways for terabit/s satellite," *International Journal of Satellite Communications and Networking*, vol. 32, no. 2, pp. 93–106, 2014.

[8] M. Muhammad, G. Giambene, T. d. Cola, M. Berioli, and N. Alagha, "Network-coding-based gateway handover scheme for terabit satellite networks," in *31st AIAA International Communications Satellite Systems Conference*, 2013.

[9] H. Skinnemoen, "Gateway diversity in ka-band systems," in *4th Ka-band Utilization Conference*, Venice, Italy, 1998.

[10] A. Gharanjik, B. S. M. R. Rao, P.-D. Arapoglou, and B. Ottersten, "Gateway switching in Q/V band satellite feeder links," *IEEE Communications Letters*, vol. 17, no. 7, pp. 1384–1387, 2013.

[11] M. Marcus and B. Pattan, "Millimeter wave propagation; spectrum management implications," *IEEE Microwave Magazine*, vol. 6, no. 2, pp. 54–62, 2005.

[12] A. Panagopoulos, P.-D. Arapoglou, and P. Cottis, "Satellite communications at KU, KA, and v bands: Propagation impairments and mitigation techniques," *IEEE Communications Surveys Tutorials*, vol. 6, no. 3, pp. 2–14, 2004.

[13] "ITU-R Recommendation P.676-10," *Attenuation by atmospheric gases*, 2013.

[14] "ITU-R Recommendation P.840-6," *Attenuation due to clouds and fog*, 2013.

[15] "ITU-R Recommendation P.618-11," *Propagation data and prediction method required for the design of the Earth-space telecommunication systems*, 2013.

[16] S. H. Lin, "Statistical behavior of rain attenuation," *Bell System Technical Journal*, vol. 52, no. 4, pp. 557–581, 1973.

[17] J. Lemorton, L. Castanet, F. Lacoste, C. Riva, E. Matricciani, U.-C. Fiebig, M. Van de Kamp, and A. Martellucci, "Development and validation of time-series synthesizers of rain attenuation for ka-band and Q/V-band satellite communication systems," *International Journal of Satellite Communications and Networking*, vol. 25, no. 6, pp. 575–601, 2007.

[18] T. Maseng and P. Bakken, "A stochastic dynamic model of rain attenuation," *IEEE Transactions on Communications*, vol. 29, no. 5, pp. 660–669, 1981.

[19] "ITU-R Recommendation P.1853-1," *Tropospheric attenuation time series synthesis*, 2012.

[20] P.-D. Arapoglou, K. P. Liolis, and A. D. Panagopoulos, "Railway satellite channel at ku band and above: Composite dynamic modeling for the design of fade mitigation techniques," *International Journal of Satellite Communications and Networking*, vol. 30, no. 1, pp. 1–17, 2012.

[21] G. A. Karagiannis, A. D. Panagopoulos, and J. D. Kanellopoulos, "Multidimensional rain attenuation stochastic dynamic modeling: Application to EarthSpace diversity systems," *Antennas and Propagation, IEEE Transactions on*, vol. 60, no. 11, pp. 5400–5411, 2012.

[22] "ITU-R Recommendation P.1815-1," *Differential rain attenuation*, 2009.

[23] J. Aitchison and J. A. C. Brown, *The Lognormal Distribution*, 1st ed. Cambridge University Press, 1957.

[24] M. Luglio, "Fade prediction and control systems," in , *1995 URSI International Symposium on Signals, Systems, and Electronics, 1995. ISSSE '95, Proceedings*, 1995, pp. 71–75.

[25] B. Gremont, M. Filip, P. Gallois, and S. Bate, "Comparative analysis and performance of two predictive fade detection schemes for ka-band fade countermeasures," *IEEE Journal on Selected Areas in Communications*, vol. 17, no. 2, pp. 180–192, 1999.

[26] A. Chambers and I. Otung, "Neural network approach to short-term fade prediction on satellite links," *Electronics Letters*, vol. 41, no. 23, pp. 1290–1292, Nov. 2005.

[27] S. M. Kay, *Fundamentals of statistical signal processing, Volume 1.* Englewood Cliffs (N.J.): Prentice Hall PTR, 1993, 00065.

[28] T. H. Cormen, C. E. Leiserson, R. L. Rivest, and C. Stein, *Introduction to Algorithms, 3rd Edition*, 3rd ed. The MIT Press, 2009.

[29] H. A. David and H. N. Nagaraja, *Order statistics.* Hoboken, NJ: Wiley-Interscience, 2003.

Ahmad Gharanjik (S'12) received a M.S. Degree in Telecommunication Systems form K. N. Toosi University of Technology, Tehran, Iran in 2010. He is currently pursuing the Ph.D. degree at both University of Luxembourg and KTH Royal Institute of Technology, Sweden. He was with Huawei Technology, Tehran from 2010 to 2012 as a WiMAX Performance Optimization Engineer.

His current research interests include signal processing for satellite communication, convex and robust optimization.

Bhavani Shankar M R (M'11) received Masters and Ph. D in Electrical Communication Engineering from Indian Institute of Science, Bangalore in 2000 and 2007, respectively. He was a Post Doc at the ACCESS Linnaeus Centre, Signal Processing Lab, Royal Institute of Technology (KTH), Sweden from 2007 to September 2009 and is currently a Research Scientist at SnT. He was with Beceem Communications, Bangalore from 2006 to 2007 as a Staff Design Engineer working on Physical Layer algorithms for WiMAX compliant chipsets. He was a visiting student at the Communication Theory Group, ETH Zurich, headed by Prof. Helmut Bölcskei during 2004. Prior to joining Ph. D, he worked on Audio Coding algorithms in Sasken Communications, Bangalore as a Design Engineer from 2000 to 2001. He is currently on the executive committee of the IEEE Benelux joint chapter on communications and vehicular technology. He was a co-recipient of the IEEE Communications Society Satellite and Space Communications Technical Committee (SSC-TC) award for Distinguished Contributions to Satellite Communications in 2014. His research interests include statistical signal processing, wireless communications, resource allocation, game theory and fast algorithms for structured matrices.

Pantelis-Daniel Arapoglou received the Diploma Degree in Electrical and Computer Engineering and the Dr. Engineering Degree from the National Technical University of Athens (NTUA), Greece, in 2003 and 2007, respectively. From September 2008 to October 2010, he was involved in postdoctoral research on MIMO over satellite jointly supported by the NTUA and the European Space Agency Research and Technology Centre (ESA/ESTEC), the Netherlands. From October 2010 to September 2011 he was a Research Associate with the Interdisciplinary Centre for Security, Reliability and Trust (SnT) of the University of Luxembourg. Since September 2011 he is a Communications System Engineer at ESA/ESTEC. His research interests include physical and link layer issues for wireless and satellite communications. Daniel is a member of the IEEE and of the Technical Chamber of Greece (TEE). In 2004 he received the "Ericsson Award of Excellence in Telecommunications" for his diploma thesis and in 2005 the URSI General Assembly Young Scientist Award. He has participated in the work of Study Group 3 of the ITU-R, in SatNEx III and in COST Action IC0802.

Björn Ottersten (S'87-M'89-SM'99-F'04) was born in Stockholm, Sweden, 1961. He received the M.S. degree in electrical engineering and applied physics from Linköping University, Linköping, Sweden, in 1986. In 1989 he received the Ph.D. degree in electrical engineering from Stanford University, Stanford, CA.

Dr. Ottersten has held research positions at the Department of Electrical Engineering, Linköping University, the Information Systems Laboratory, Stanford University, the Katholieke Universiteit Leuven, Leuven, and the University of Luxembourg. During 96/97 Dr. Ottersten was Director of Research at ArrayComm Inc, a start-up in San Jose, California based on Otterstens patented technology. He has co-authored journal papers that received the IEEE Signal Processing Society Best Paper Award in 1993, 2001, 2006, and 2013 and 3 IEEE conference papers receiving Best Paper Awards. In 1991 he was appointed Professor of Signal Processing at the Royal Institute of Technology (KTH), Stockholm. From 1992 to 2004 he was head of the department for Signals, Sensors, and Systems at KTH and from 2004 to 2008 he was dean of the School of Electrical Engineering at KTH. Currently, Dr. Ottersten is Director for the Interdisciplinary Centre for Security, Reliability and Trust at the University of Luxembourg. Dr. Ottersten is a board member of the Swedish Research Council and as Digital Champion of Luxembourg, he acts as an adviser to the European Commission.

Dr. Ottersten has served as Associate Editor for the IEEE TRANSACTIONS ON SIGNAL PROCESSING and on the editorial board of *IEEE Signal Processing Magazine*. He is currently editor in chief of *EURASIP Signal Processing Journal* and a member of the editorial boards of *EURASIP Journal of Applied Signal Processing and Foundations and Trends in Signal Processing*. Dr. Ottersten is a Fellow of the IEEE and EURASIP and a member of the IEEE Signal Processing Society Board of Governors. In 2011 he received the IEEE Signal Processing Society Technical Achievement Award. He is a first recipient of the European Research Council advanced research grant. His research interests include security and trust, reliable wireless communications, and statistical signal processing.